PAPER

Check for updates

An improved mechanistic model for the diastereoselective addition of Grignard reagents to *N*-(*tert*-butylsulfinyl)imines

David Guijarro [ID]

The mechanism of the diastereoselective addition of ethylmagnesium bromide to (*S*)-*N*-benzylidene-2-methylpropane-2-sulfinamide in CH_2Cl_2 has been studied by DFT calculations using a model that involves an explicit molecule of diethyl ether (coming from the Grignard reagent solution) coordinated to the magnesium atom. Several reaction pathways have been investigated and the energy profiles obtained for the preferred routes lead to an estimated diastereomeric ratio that matches very well with the experimental data. This new mechanistic model gives a plausible explanation of the diastereoselectivity obtained in the reaction.

Introduction

The diastereoselective addition of alkyl Grignard reagents to the C=N bond of enantiomerically pure *N*-(*tert*-butylsulfinyl)imines leads to chiral sulfinamides that can be easily desulfinylated to give α-branched primary amines,[1] which are valuable intermediates in pharmaceuticals and fine chemicals. The steric and electronic effects imparted by the *tert*-butylsulfinyl group can significantly influence the reaction pathway, enhancing the diastereoselectivity of the addition process. The knowledge of the mechanism of the reaction is crucial to understand how reactants transform into products, which can help to find the factors influencing the stereoselectivity and to facilitate the determination of the optimum reaction conditions. Ellman *et al.* studied the addition of Grignard reagents to this type of imines.[2] They found that the stereoselectivity depended on the solvent used and proposed a tentative transition structure that predicted the stereochemical outcome of the reaction.

Computational chemistry has shown to be a powerful toolkit for exploring the mechanistic pathways and energetics of organic reactions. By employing methods such as density functional theory (DFT) calculations, we can gain insights into transition structures, intermediate species and energy profiles of a variety of processes. Such computational studies can complement the experimental efforts to find the mechanism of a reaction and can also provide predictive capabilities that could lead to the design of more efficient synthetic routes. The mechanism of the addition of MeMgBr to (*S*)-*N*-benzylidene-2-methylpropane-2-sulfinamide has been studied by DFT calculations by Eisenstein *et al.*[3] Solvation effects (THF) were

evaluated by the SMD method, not including explicit solvent molecules in their mechanistic model. Although their results indicate that the sulfinamide with the (S_S,R)-configuration would be the preferred diastereoisomer, the difference of 9.0 kcal mol^{-1} between the transition structures corresponding to the two diastereomeric products suggests that the (S_S,R)-product would be exclusively formed, which is not in agreement with the experimental diastereomeric ratio (S_S,R) : (S_S,S) of 93 : 7. As part of one of our ongoing research projects, I was interested in trying to find a mechanistic model for the addition of EtMgBr to the (*S*)-*N*-benzylidene-2-methylpropane-2-sulfinamide that more closely fitted the experimentally obtained results. Since Ellman *et al.* found that the best diastereoselectivities were obtained using CH_2Cl_2 as solvent, I decided to perform theoretical calculations in that medium. Considering that a solution of EtMgBr in Et_2O was used in Ellman's experiment, the coordination of a molecule of Et_2O to the magnesium atom in the transition structure would be very likely. Thus, I thought about a mechanistic model that included an explicit molecule of Et_2O. The results of this comprehensive computational study are presented herein.

Computational details

The geometry optimizations were performed by DFT calculations with the program package Gaussian 16, revision C.01,[4] using the B3LYP functional[5] with D3 dispersion correction[6] and the 6-31G(d,p) basis set.[7] The effect of the bulk solvent CH_2Cl_2 ($\varepsilon = 8.93$) was estimated by using the Solvation Model based on Density (SMD).[8] Vibrational frequency calculations were carried out at the same level of theory and they confirmed that the optimized structures were either minima (no imaginary frequencies) or transition structures (only one imaginary frequency) on the potential energy surfaces (PES). For each

Departamento de Química Orgánica, Facultad de Ciencias and Instituto de Síntesis Orgánica (ISO), Universidad de Alicante, Apdo. 99, 03080 Alicante, Spain. E-mail: dguijarro@ua.es

transition structure, the intrinsic reaction coordinate (IRC)[9] routes towards the corresponding minima were calculated and, if the IRC calculations failed to reach the energy minima, geometry optimizations were performed from the final point of the IRC analysis. Gibbs free energies at 298.15 K and at 225.15 K were calculated by the addition of the thermal corrections to Gibbs free energy obtained from the vibrational frequency calculations of the geometries optimized at B3LYP-D3/6-31G(d,p) level with the electronic energies obtained from single-point calculations of the optimized geometries with the M06-2X functional[10] and the 6-311G(d,p) basis set.[7] A correction term of 1.89 kcal mol^{-1} (for calculations at 298.15 K) or 1.31 kcal mol^{-1} (for calculations at 225.15 K) was added to the Gibbs free energies obtained before in order to consider the change in the standard state from 1 atm to 1 M. The study of non-covalent interactions was done using the application NCIWEB.[11]

Results and discussion

I was interested in performing a theoretical study on the mechanism of the addition of EtMgBr to (S)-N-(tert-butylsulfinyl)imine **1** that could provide a reasonable explanation for the diastereoselectivity obtained experimentally (Scheme 1).[12]

First, I decided to evaluate the effect of the solvent on the diastereoselectivity in the model that was studied by Eisenstein et al. for the addition of MeMgBr to the same imine,[3] since they used THF and I was interested in the reaction in CH$_2$Cl$_2$. From the possible routes studied by them, I chose the transition structure with lowest energy for the formation of every diastereomeric product and applied a similar model for the formation of addition products **2** and **3** (Scheme 1). The two pathways that I studied are depicted in Scheme 2, in which tentative forms for the transition structures **TS 1-2** and **TS 1-3** have been included. DFT calculations [B3LYP-D3/6-31G(d,p)] were performed considering solvent effects in CH$_2$Cl$_2$ by the SMD method. The geometries of the obtained transition structures are shown in Fig. 1. Both **TS 1-2** and **TS 1-3** show a boat-like arrangement for the six atoms involved in the reaction. The magnesium atom is coordinated to the oxygen atom of the sulfinyl group, approaching the ethyl group to the electrophilic carbon of the imine. After performing an intrinsic reaction coordinate (IRC) analysis, the corresponding reactive complexes **R2** (for **TS 1-2**) and **R3** (for **TS 1-3**) were obtained (see Fig. 1). Both **R2** and **R3** present an s-trans geometry in the imine moiety and are formed by coordination of the magnesium atom to the oxygen atom of the sulfinyl group, differing in the spatial orientation of the Br

atom and the Et group in relation to a hypothetical plane containing N, S, O and Mg atoms.

Fig. 1 shows the energy profiles and the optimized molecular structures[13] for the two possible reaction pathways. The starting point are separated EtMgBr and the imine with the s-cis conformation **1′**.[14] The imine would change its conformation to s-trans **1**, which is only 4.2 kcal mol^{-1} higher in energy and it is the precursor of the reactive complexes. Coordination of EtMgBr to **1** leads to the two possible reactive complexes **R2** and **R3** with a considerable fall in energy (21.0 and 20.8 kcal mol^{-1}, respectively). **R2** and **R3** are almost isoenergetic. The addition reaction is thermodynamically favored in both cases. The activation barrier for the formation of **2** (16.7 kcal mol^{-1}) is considerably lower than the one for the generation of **3** (23.9 kcal mol^{-1}). The difference between these two activation barriers is 7.2 kcal mol^{-1}, which suggests that only product **2** with the R-configuration in the stereogenic carbon atom would be formed, which is not in agreement with the experimental diastereomeric ratio of 92 : 8. Therefore, the change of the solvent from THF (Eisenstein et al.[3]) to CH$_2$Cl$_2$ (this work) leads to the same conclusion that the (S$_S$,S) diastereoisomer should not be detected, which is not the case. Since the s-cis conformation of imine **1′** is more stable than the s-trans, I also studied two more reactive complexes with the s-cis conformation, but their energies were almost the same as the ones of **R2** and **R3**, not leading to any significant variation of the reaction barriers to reach **TS 1-2** and **TS 1-3** (see the SI for details). These results encouraged me to try to find another mechanistic model that would better fit the experimental diastereoselectivity.

Considering that a solution of EtMgBr in Et$_2$O was used in Ellman's experiment, the coordination of a molecule of Et$_2$O to the magnesium atom in the reactive complex, in the transition structure and in the product would be very likely. Therefore, I contemplated the introduction of an explicit molecule of Et$_2$O to the mechanistic model.[15] Although the E imine mainly exists in its s-cis form **1′** in solution in CH$_2$Cl$_2$, since the barrier for its conversion to the s-trans form **1** is only 6.4 kcal mol^{-1} (see the SI for details), I considered reactive complexes **4′** and **6** (Schemes 3 and 4) as possible precursors of the addition products. On the other hand, although the Z imines are more unstable than **1′** or **1**, I also contemplated possible routes to the addition products through transition structures involving an imine moiety with Z configuration in order to check if the formation of the reactive complexes had any influence on the kinetics for the isomerization of the C=N bond via nitrogen inversion.
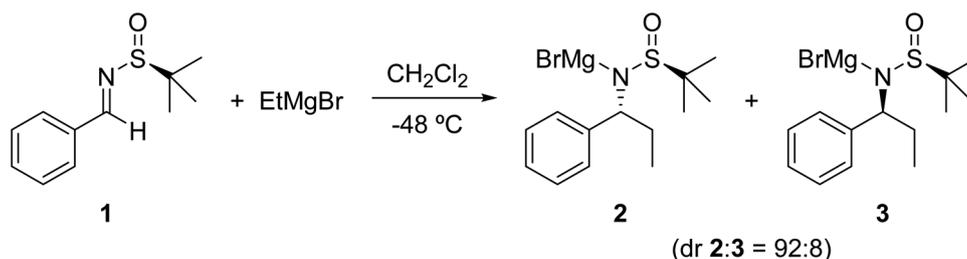
Scheme 1 Reaction for the theoretical study performed in this work.
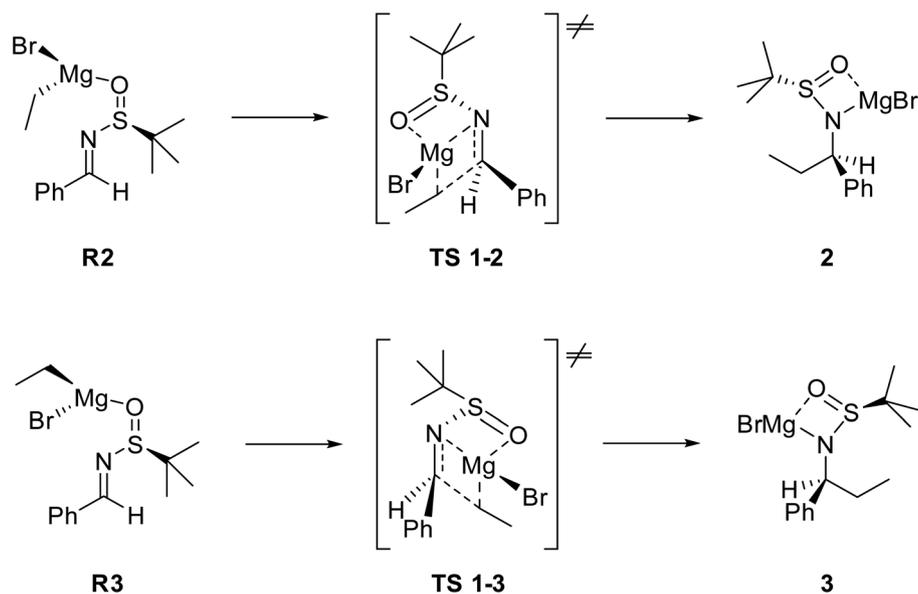
Scheme 2 Reaction pathways studied for the addition of EtMgBr to imine **1** without the participation of Et₂O molecules.

First, DFT calculations showed the thermodynamic feasibility of the generation of reactive complexes with a coordinated molecule of Et₂O **4′** and **6** (see the SI for details), which differ in the conformation of the imine moiety. I envisioned two alternative routes for the conversion of **4′** into the (*S*) addition product **5** (Scheme 3). The most direct way is the generation of
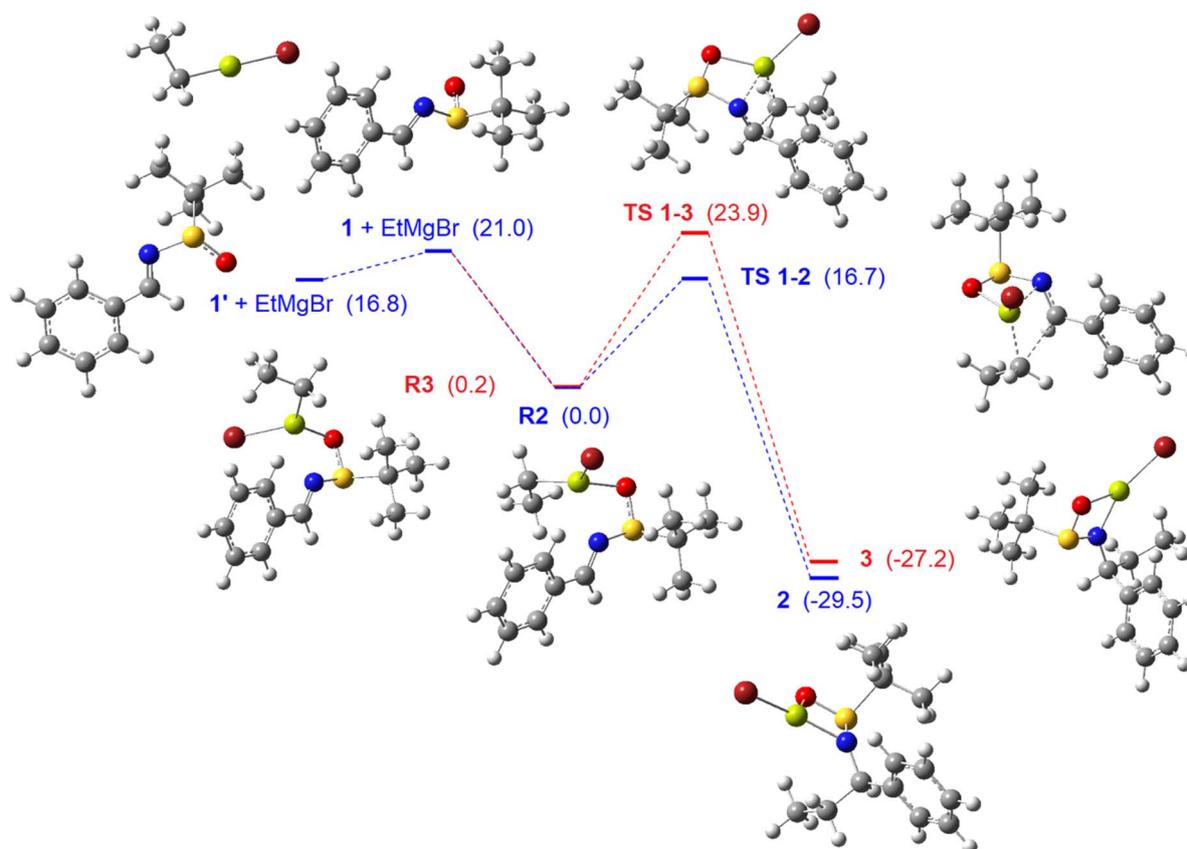

Fig. 1 Optimized structures and energy profiles for the two possible reaction pathways for the addition of EtMgBr to imine **1**, obtained from DFT calculations [geometry optimizations at B3LYP-D3/6-31G(d,p) level and energies by single-point calculations at M06-2X/6-311G(d,p) level, both in CH₂Cl₂ at 298.15 K] (color of atoms: C, grey; H, white; N, blue; O, red; S, yellow; Mg, green; Br, dark red). Relative Gibbs free energy values are given in brackets (kcal mol⁻¹). **1′** is the *E* imine with s-*cis* conformation and **1** is the *E* imine with s-*trans* conformation. Reactive complex **R2** was taken as zero-energy.
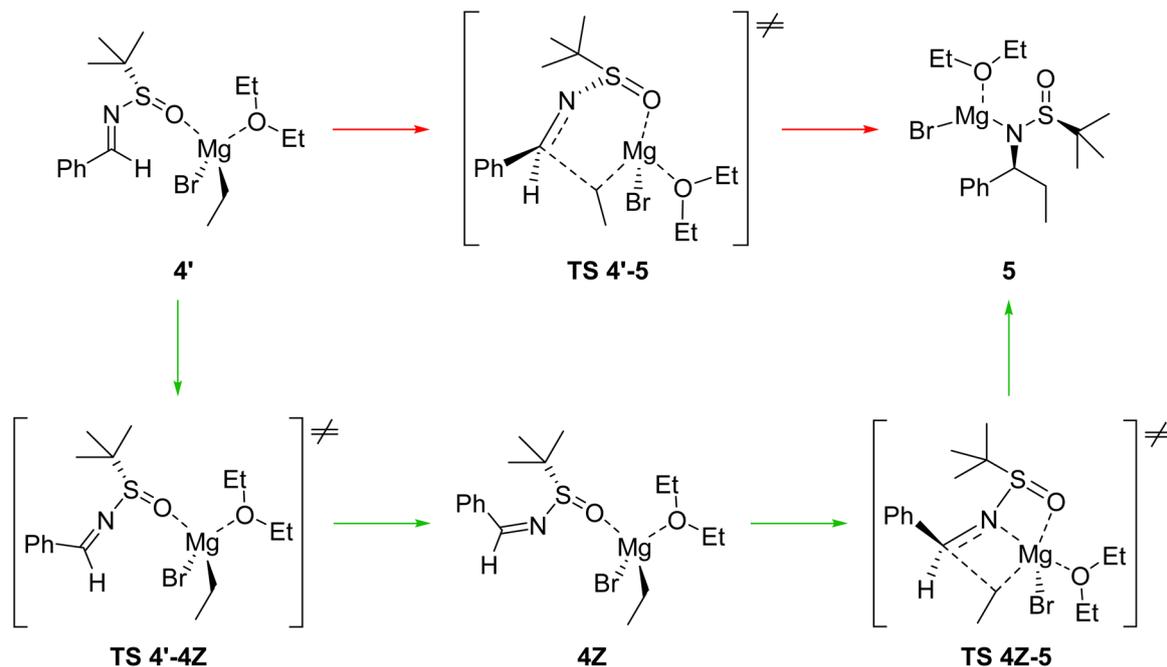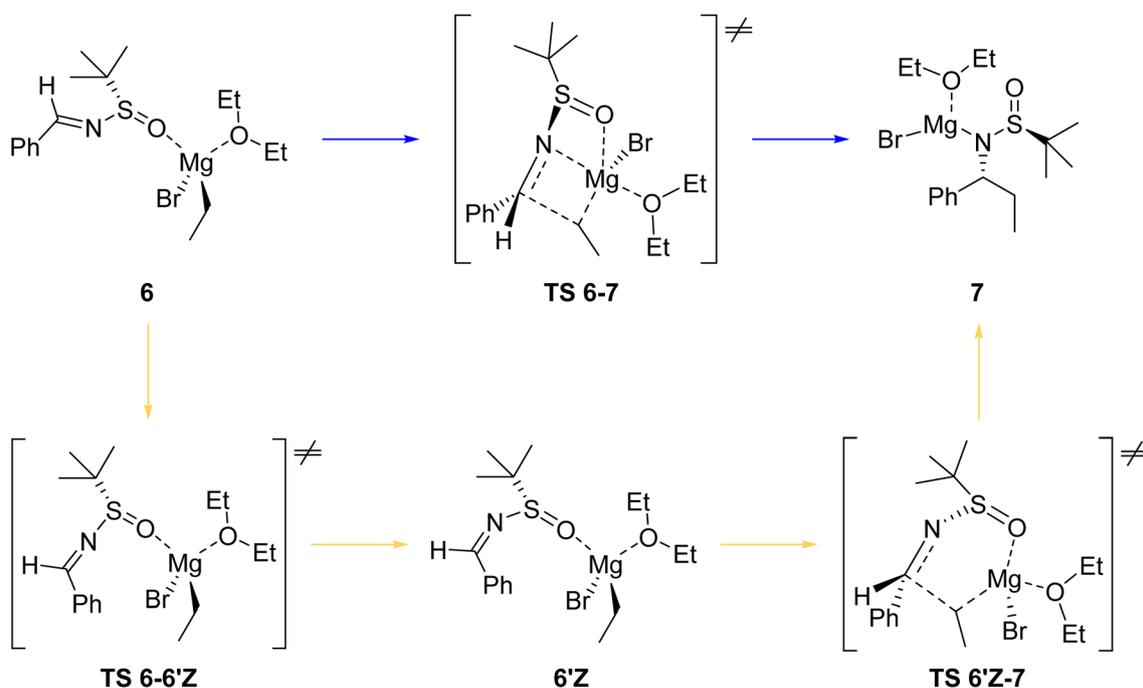
Scheme 3 Possible reaction routes for the transformation of **4′** into the (*S*) addition product **5**.

TS 4′-5, which would then evolve to the final product **5** (red arrows in Scheme 3). The second approach involves isomerization of the C=N bond by inversion of the N atom, giving structure **4Z** through **TS 4′-4Z**, followed by formation of the transition structure for the addition step, **TS 4Z-5**, and evolution to product **5** (green arrows in Scheme 3).

Fig. 2 shows the energy profiles for these two routes and the optimized geometries of all the species that participate.

Complex **4′** could isomerize to **4Z** by inversion of the N atom *via* transition structure **TS 4′-4Z**, which is 20.0 kcal mol^{-1} higher in energy than **4′** and in which the C=N–S subunit presents an almost linear geometry (angle 165.5°). The transition structure for the transfer of the ethyl group from Mg to the iminic carbon, **TS 4Z-5**, could then be formed and the atoms involved in the reaction show a boat-like shape, with a probable coordination of the N atom to Mg. This transition structure lies 20.9 kcal mol^{-1}

Scheme 4 Possible reaction routes for the transformation of **6** into the (*R*) addition product **7**.
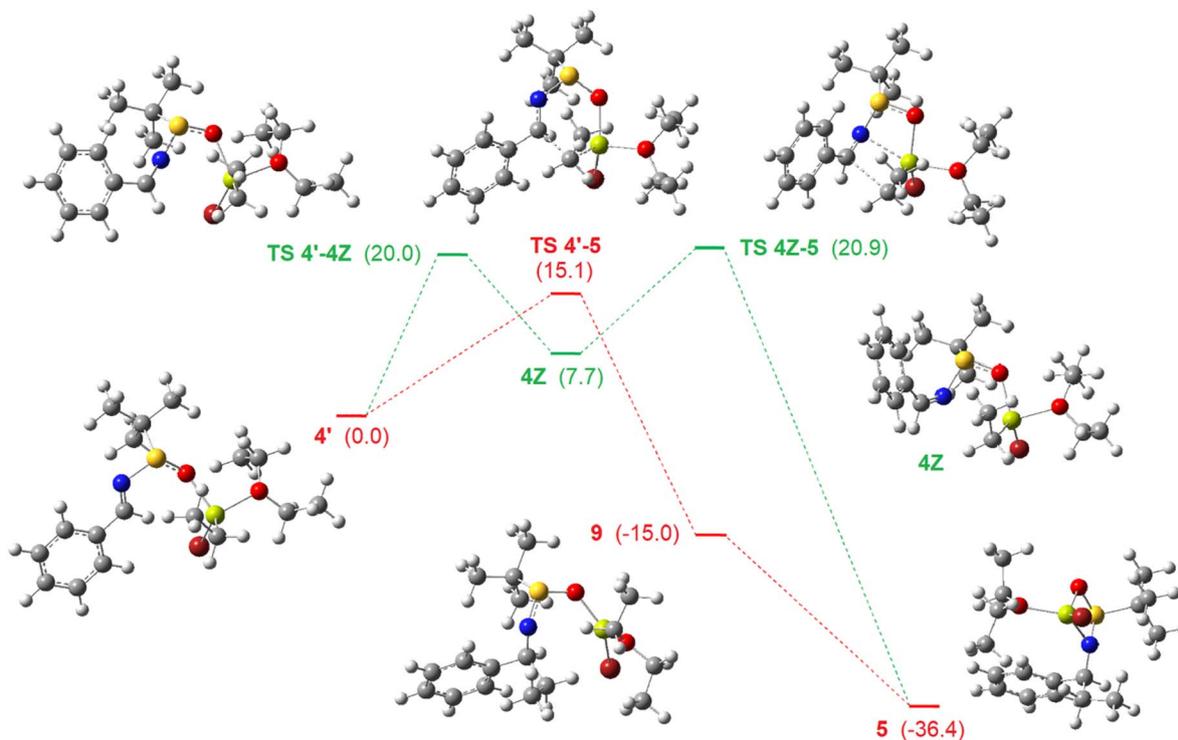
RSC Advances

Paper

Fig. 2 Optimized structures and energy profiles for the two possible reaction pathways for the conversion of **4′** into **5**, obtained from DFT calculations [geometry optimizations at B3LYP-D3/6-31G(d,p) level and energies by single-point calculations at M06-2X/6-311G(d,p) level, both in CH$_2$Cl$_2$ at 298.15 K] (color of atoms: C, grey; H, white; N, blue; O, red; S, yellow; Mg, green; Br, dark red). Relative Gibbs free energy values are given in brackets (kcal mol^{-1}). Reactive complex **4′** was taken as zero-energy.

above **4′**. Creation of the ethyl–carbon bond leads to the final (S) addition product **5**, which is 36.4 kcal mol^{-1} more stable than **4′**. In product **5**, N, S, O and Mg atoms form a four-membered ring by coordination of the sulfinyl O to Mg.

On the red pathway, complex **4′** directly leads to the transition structure for the addition reaction, **TS 4′-5**, which is 15.1 kcal mol^{-1} higher in energy than **4′**. When it evolves to the addition product, a stationary point is found with structure **9** (see Fig. 2), in which N and Mg atoms are quite separated from each other (distance 3.38 Å). Species **9** is 21.4 kcal mol^{-1} higher in energy than the addition product **5**, which indicates that coordination of Mg to both N and the O of the sulfinyl group highly stabilizes the addition product. In fact, starting from **9**, approaching Mg to N and performing an optimization of the geometry led to product **5**. This red route has a lower barrier (15.1 kcal mol^{-1}) than the green one (20.9 kcal mol^{-1}), the difference between them being 5.8 kcal mol^{-1}, which suggests that the formation of product **5** will occur exclusively through **TS 4′-5**.

Concerning the transformation of complex **4′** into the (R) addition product **7**, two alternative routes were also planned (Scheme 4). First, **4′** could easily change its conformation to the s-trans arrangement of **6**. From reactive complex **6**, the shortest way would be generation of transition structure **TS 6-7** and evolution to product **7** (blue arrows in Scheme 4). The other proposed route requires the isomerization of the C=N bond to give complex **6′Z** through transition structure **TS 6-6′Z**, followed by formation of the transition structure for the addition of the

ethyl group by the Re face of the iminic carbon, **TS 6′Z-7**, that would finally give product **7** (yellow arrows in Scheme 4).

The energy profiles for these two pathways and the optimized geometries obtained from the DFT calculations are depicted in Fig. 3. The variation of the dihedral angle C=N–S=O of reactive complex **4′** to the s-trans structure **6** should be very easy, with a barrier of only 3.2 kcal mol^{-1}. Complex **6** is only 1.2 kcal mol^{-1} less stable than **4′**. Partial creation of the new bond between the ethyl group and the iminic carbon, together with coordination of the N atom to Mg, leads to the boat-like transition structure **TS 6-7**, which lies 13.8 kcal mol^{-1} above **4′** and evolves directly to the (R) addition product **7**. This product is isoenergetic with its diastereoisomer **5** and presents the same coordination of the O of the sulfinyl group to Mg as the latter.

The alternative yellow route from **6** to **7** is a two-step process. First, **6** isomerizes to **6′Z** by inversion of the N atom through transition structure **TS 6-6′Z**, which is 19.8 kcal mol^{-1} higher in energy than **4′**. The barrier for this isomerization is almost identical to the one found before in the transformation **4′** → **4Z** (see Fig. 2) and a quasi-linear arrangement of iminic carbon, N and S atoms is also observed in **TS 6-6′Z** (angle 174.5°, Fig. 3). The transfer of the ethyl group takes place from the complex with a Z imine moiety **6′Z**, to give the final product **7** through transition structure **TS 6′Z-7**. The barrier for this two-step process (27.9 kcal mol^{-1}) is much higher than the one for the blue profile in Fig. 3 (13.8 kcal mol^{-1}). Therefore, the conversion of **4′** to **7** through **TS 6-7** is kinetically much more favored.

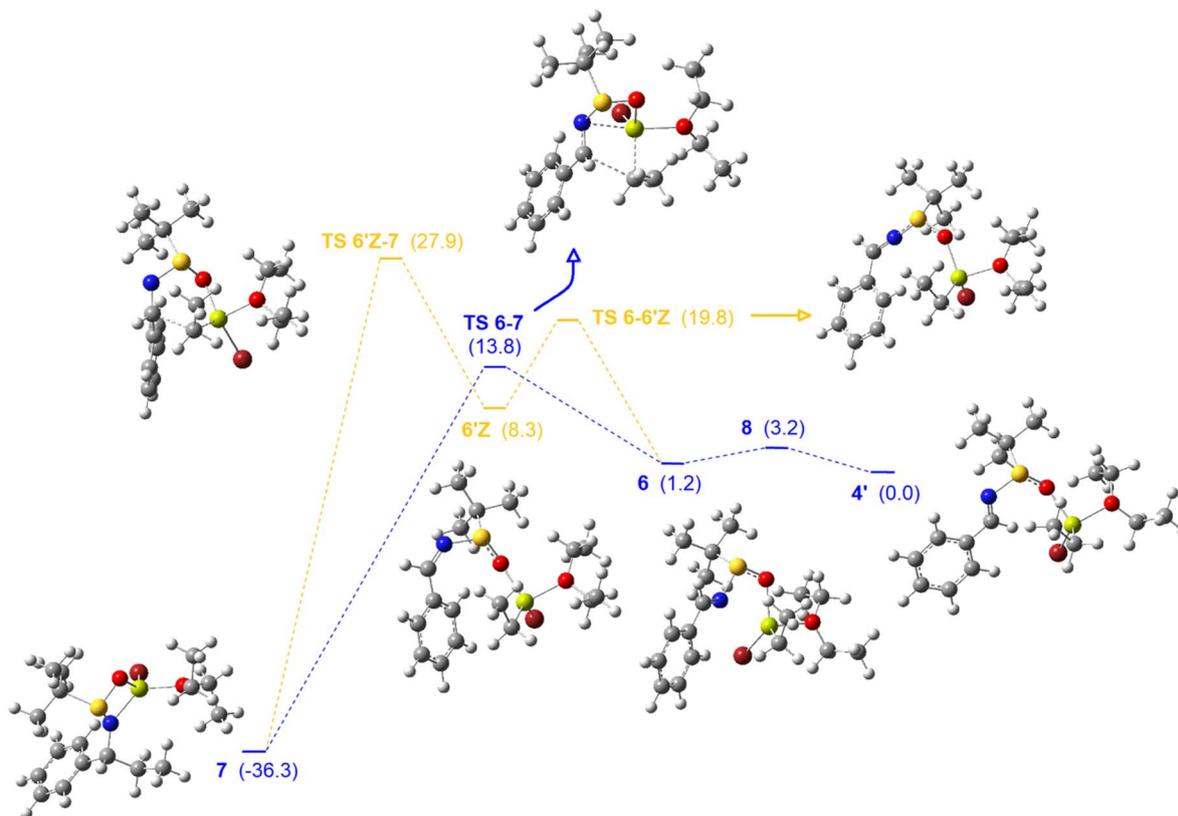**Fig. 3** Optimized structures and energy profiles for the two possible reaction pathways for the conversion of **4'** into **7**, obtained from DFT calculations [geometry optimizations at B3LYP-D3/6-31G(d,p) level and energies by single-point calculations at M06-2X/6-311G(d,p) level, both in CH_2Cl_2 at 298.15 K] (color of atoms: C, grey; H, white; N, blue; O, red; S, yellow; Mg, green; Br, dark red). Relative Gibbs free energy values are given in brackets (kcal mol^{-1}). Reactive complex **4'** was taken as zero-energy.

The transition structures of lowest energy for the formation of every diastereomeric product, **TS 4'-5** and **TS 6-7** are shown together in Fig. 4 for an easier comparison of them. The six atoms of **TS 4'-5** involved in the reaction show a cyclohexene-like half-chair structure. Atoms N, S, O1 and Mg are almost coplanar (dihedral angle 3.7°), C1 is located below that plane (dihedral angle C1–N–S–O1 −21.3°) and C2 is above that plane (dihedral angle S–O1–Mg–C2 −32.8°). **TS 6-7** is a boat-like transition structure in which C1, C2, S and O1 act as in-plane atoms and N and Mg act as out-of-plane atoms. The short N–Mg distance (2.47 Å) suggests that there is a coordination between these two atoms, which may stabilize the transition structure. The possibility of having this N–Mg interaction could be an important factor influencing the relative energies of the transition structures, since the Mg atom is coordinated to both N and O1 in both products **5** and **7** (see Fig. 2 and 3). Due to that N–Mg interaction, Mg atom in **TS 6-7** is pentacoordinated,[16] with a slightly distorted trigonal bipyramidal structure in which N and O2 occupy the apical positions and C2, O1 and Br occupy the equatorial positions (see Fig. 4). In **TS 4'-5**, the N–Mg distance (3.24 Å) is quite longer than in **TS 6-7** and the interaction between these two atoms seems not to be possible in the former, since the Mg atom is tetracoordinated with a quasi-tetrahedral structure (see some relevant angles around Mg in **TS 4'-5** in Fig. 4).

With the aim of trying to get more insight about the source of the difference in energy between the two transition structures, an investigation of non-covalent interactions[17] was performed and they are represented in Fig. 5. Both transition structures show strong attractive interactions between Mg and the O of the Et_2O molecule, the O of the sulfinyl group and the Br atom. Moreover, **TS 6-7** shows a weak attractive Mg–N interaction, which supports the idea that a coordination between these two atoms has already started in the transition structure, giving it a boat-like shape. This Mg–N interaction can contribute to the stabilization of **TS 6-7** in relation to **TS 4'-5**, in which it is not observed.

The deformation energy and the interaction energy[18] for both transition structures have also been computed considering two interacting subunits: the sulfinyl imine on one hand and the Grignard reagent coordinated to the Et_2O molecule on the other hand (see the SI for details). The obtained results are shown in Fig. 6. The interaction energy for **TS 4'-5** is higher than the one for **TS 6-7**. This is reflected in the distances between the interacting atoms, which are shorter in the former transition structure [C1–C2 = 2.28 Å (for **TS 4'-5**) and 2.43 Å (for **TS 6-7**); O1–Mg = 1.96 Å (for **TS 4'-5**) and 2.02 Å (for **TS 6-7**); see atom labels in Fig. 4]. Concerning the deformation energy, it is also considerably higher for **TS 4'-5** than for **TS 6-7** (Fig. 6). Comparing the geometries of the two transition structures and **4'**, we can see
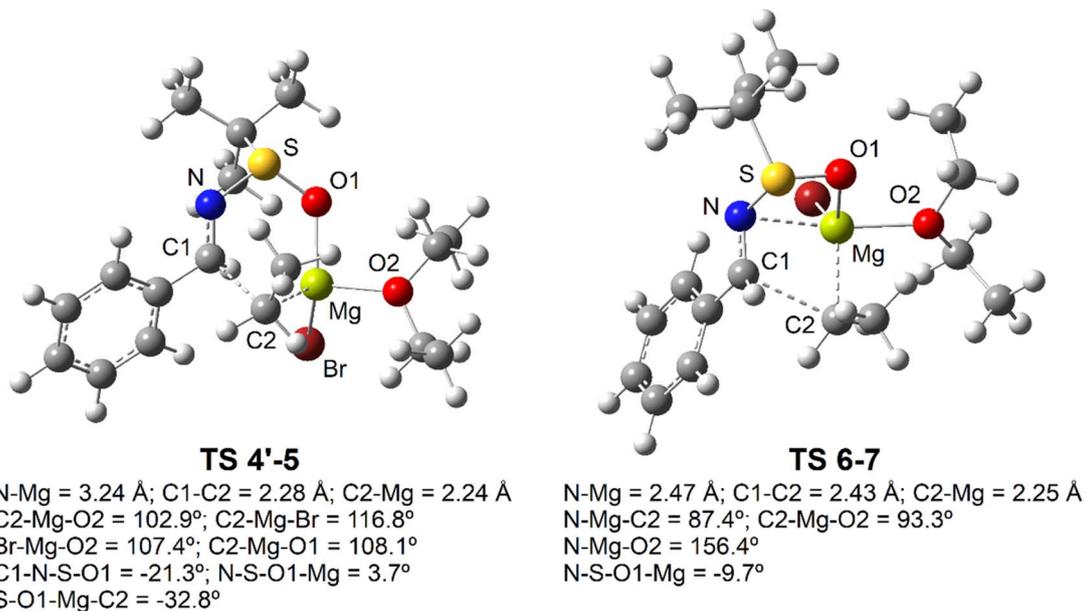
TS 4'-5

N–Mg = 3.24 Å; C1–C2 = 2.28 Å; C2–Mg = 2.24 Å
C2–Mg–O2 = 102.9°; C2–Mg–Br = 116.8°
Br–Mg–O2 = 107.4°; C2–Mg–O1 = 108.1°
C1–N–S–O1 = −21.3°; N–S–O1–Mg = 3.7°
S–O1–Mg–C2 = −32.8°

TS 6-7

N–Mg = 2.47 Å; C1–C2 = 2.43 Å; C2–Mg = 2.25 Å
N–Mg–C2 = 87.4°; C2–Mg–O2 = 93.3°
N–Mg–O2 = 156.4°
N–S–O1–Mg = −9.7°

Fig. 4   Comparison of the optimized structures **TS 4′-5** and **TS 6-7**. (Color of atoms: C, grey; H, white; N, blue; O, red; S, yellow; Mg, green; Br, dark red).
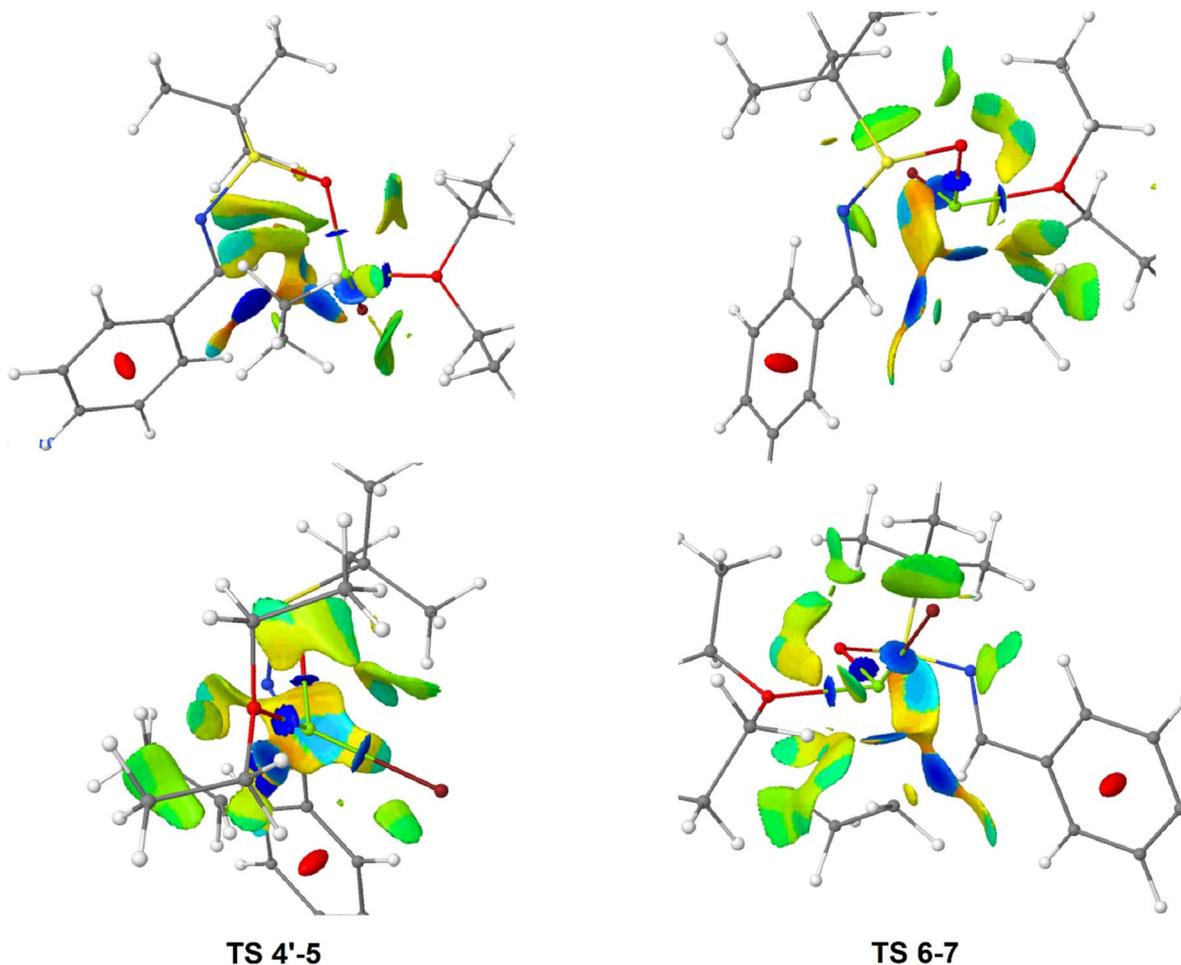

TS 4'-5

TS 6-7

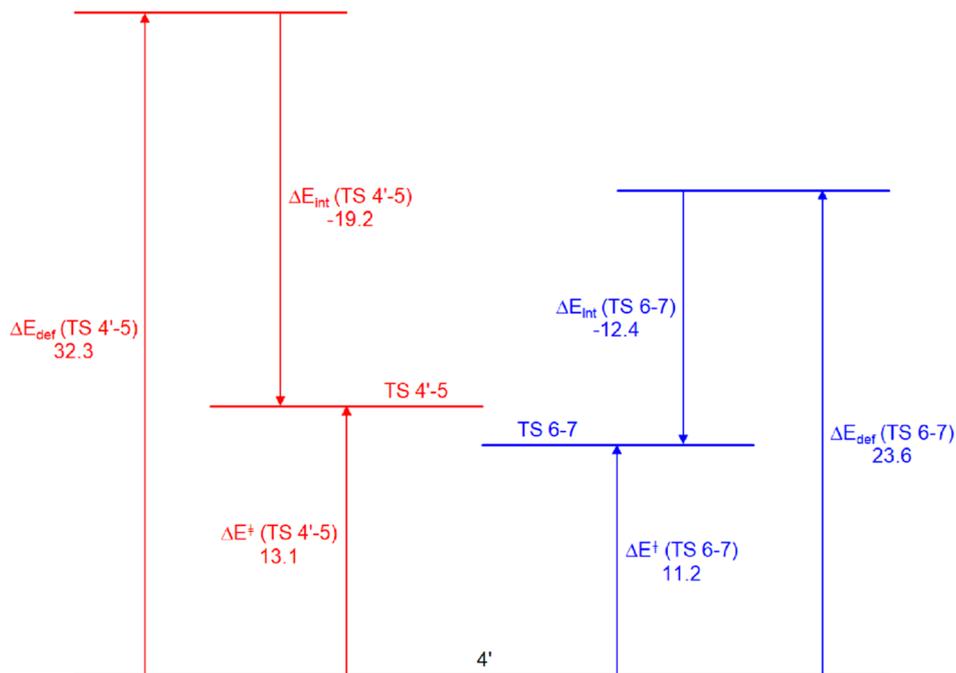Fig. 5   Representation of non-covalent interactions found in **TS 4′-5** and **TS 6-7**.

Fig. 6 Representation of the activation, the deformation and the interaction energies of transition structures **TS 4′-5** and **TS 6-7**, obtained from single-point calculations at M06-2X/6-311G(d,p) level in CH_2Cl_2 at 298.15 K. Energy values are given in kcal mol^{-1}.

some features that could contribute to the difference in the deformation energies of the two transition structures: (a) the angle Ph–(CN)–H is almost equal for **4′** and **TS 6-7** (115.2° and 115.7°, respectively), while it is narrower for **TS 4′-5** (110.2°); (b) the distance between the iminic H and the closest H of the *tert*-butyl group is 3.00 Å for **4′**, being shorter in **TS 4′-5** (2.27 Å, higher steric hindrance) and longer in **TS 6-7** (4.21 Å, lower steric hindrance); (c) the dihedral angle between the iminic carbon atom and the *tert*-butyl group is 108.0° in **TS 4′-5** and 165.0° in **TS 6-7**, being in an almost antiperiplanar arrangement in the latter (less steric hindrance). The fact that the difference between **TS 4′-5** and **TS 6-7** in the deformation energies (8.7 kcal mol^{-1}) is bigger than in the interaction energies (−6.8 kcal mol^{-1}) determines de final energy order of the transition structures.

As it can be seen in Fig. 2 and 3, there is a big fall in energy from the favored transition structures to the addition products (51.5 kcal mol^{-1} for **TS 4′-5** and 50.1 kcal mol^{-1} for **TS 6-7**), and this step can be considered irreversible. Therefore, it seems that the diastereoselectivity is governed by a kinetic control. The reactions of formation of both addition products are very exergonic: **5** and **7** are 36.3 kcal mol^{-1} more stable than **4′**. The addition of EtMgBr to *N*-(*tert*-butylsulfinyl)benzaldimine in CH_2Cl_2 is thus a thermodynamically favoured process.

The difference between the activation barrier to overcome **TS 4′-5** and the one for **TS 6-7** is 1.3 kcal mol^{-1}, which corresponds to a diastereomeric ratio $(S_S,R):(S_S,S)$ of 90 : 10. This value is very close to the experimental result of 92 : 8. Therefore, the new mechanistic model that has been developed here fits quite well the diastereoselectivity obtained experimentally.

In order to evaluate the effect of the temperature in the computational study, since the experimental diastereomeric ratio of 92 : 8 had been obtained in a reaction performed at −48 °C, geometry optimizations and Gibbs free energy calculations for all the species involved in the red route of Fig. 2 and the blue pathway of Fig. 3 were repeated considering a temperature of 225.15 K.[19] The geometries obtained at that temperature were practically identical to the ones that had been represented in Fig. 2 and 3. Using the new energy values at that temperature, the two activation barriers to overcome transition structures **TS 4′-5** (14.5 kcal mol^{-1}) and **TS 6-7** (13.0 kcal mol^{-1}) differ now in 1.5 kcal mol^{-1}, which leads to a calculated diastereomeric ratio $(S_S,R):(S_S,S)$ of 93 : 7 that matches very well the experimental result.

Conclusions

In conclusion, the results presented herein show that the introduction of an explicit molecule of diethyl ether coordinated to the magnesium atom in the mechanistic model for the diastereoselective addition of EtMgBr to the *N*-(*tert*-butylsulfinyl)imine derived from benzaldehyde in CH_2Cl_2 considerably improves the match between the theoretical and the experimental diastereomeric ratios.[20] The model studied in this work seems to be plausible and could help to understand the stereochemical outcome of this kind of reactions. These results reinforce the fact that the solvent could actively participate in a reaction and it should be taken into account when a theoretical mechanistic study of a reaction is being conducted.

Conflicts of interest

There are no conflicts to declare.

Data availability

Supplementary information: The data supporting this article have been included as part of the SI. Study of the structure of the imine. Other reactive complexes between the imine and EtMgBr without a Et$_2$O molecule. Thermodynamic study of the formation of reactive complexes **4′** and **6**. Calculation of the deformation energies and the interaction energies for transition structures **TS 4′-5** and **TS 6-7**. Figures, cartesian coordinates and energies of all the optimized geometries. See DOI: **https://doi.org/10.1039/d4ra06560c**.

Acknowledgements

References

1 For reviews, see: (*a*) D. Morton and R. A. Stockman, Chiral non-racemic sulfinimines: versatile reagents for asymmetric synthesis, *Tetrahedron*, 2006, **62**, 8869–8905; (*b*) F. Ferreira, C. Botuha, F. Chemla and A. Pérez-Luna, tert-Butanesulfinimines: structure, synthesis and synthetic applications, *Chem. Soc. Rev.*, 2009, **38**, 1162–1186; (*c*) M. T. Robak, M. A. Herbage and J. A. Ellman, Synthesis and Applications of tert-Butanesulfinamide, *Chem. Rev.*, 2010, **110**, 3600–3740.

2 D. A. Cogan, G. Liu and J. A. Ellman, Asymmetric synthesis of chiral amines by highly diastereoselective 1,2-additions of organometallic reagents to N-tert-butanesulfinyl imines, *Tetrahedron*, 1999, **55**, 8883–8904.

3 M. Hennum, H. Fliegl, L.-L. Gundersen and O. Eisenstein, Mechanistic Insights on the Stereoselective Nucleophilic 1,2-Addition to Sulfinyl Imines, *J. Org. Chem.*, 2014, **79**, 2514–2521.

4 M. J. Frisch, G. W. Trucks, H. B. Schlegel, G. E. Scuseria, M. A. Robb, J. R. Cheeseman, G. Scalmani, V. Barone, G. A. Petersson, H. Nakatsuji, X. Li, M. Caricato, A. V. Marenich, J. Bloino, B. G. Janesko, R. Gomperts, B. Mennucci, H. P. Hratchian, J. V. Ortiz, A. F. Izmaylov, J. L. Sonnenberg, D. Williams-Young, F. Ding, F. Lipparini, F. Egidi, J. Goings, B. Peng, A. Petrone, T. Henderson, D. Ranasinghe, V. G. Zakrzewski, J. Gao, N. Rega, G. Zheng, W. Liang, M. Hada, M. Ehara, K. Toyota, R. Fukuda, J. Hasegawa, M. Ishida, T. Nakajima, Y. Honda, O. Kitao, H. Nakai, T. Vreven, K. Throssell, J. A. Montgomery Jr, J. E. Peralta, F. Ogliaro, M. J. Bearpark, J. J. Heyd, E. N. Brothers, K. N. Kudin, V. N. Staroverov, T. A. Keith, R. Kobayashi, J. Normand, K. Raghavachari, A. P. Rendell, J. C. Burant, S. S. Iyengar, J. Tomasi, M. Cossi, J. M. Millam, M. Klene, C. Adamo, R. Cammi, J. W. Ochterski, R. L. Martin, K. Morokuma, O. Farkas, J. B. Foresman and D. J. Fox, *GAUSSIAN 16 (Revision C.01)*, Gaussian Inc., Wallingford, CT, 2019.

5 A. D. Becke, Density-functional thermochemistry. III. The role of exact exchange, *J. Chem. Phys.*, 1993, **98**, 5648–5652.

6 S. Grimme, J. Antony, S. Ehrlich and H. Krieg, A consistent and accurate ab initio parametrization of density functional dispersion correction (DFT-D) for the 94 elements H-Pu, *J. Chem. Phys.*, 2010, **132**, 154104.

7 (*a*) R. Krishnan, J. S. Binkley, R. Seeger and J. A. Pople, Self-consistent molecular orbital methods. XX. A basis set for correlated wave functions, *J. Chem. Phys.*, 1980, **72**, 650–654; (*b*) A. D. McLean and G. S. Chandler, Contracted Gaussian basis sets for molecular calculations. I. Second row atoms, Z=11–18, *J. Chem. Phys.*, 1980, **72**, 5639–5648.

8 A. V. Marenich, C. J. Cramer and D. G. Truhlar, Universal Solvation Model Based on Solute Electron Density and on a Continuum Model of the Solvent Defined by the Bulk Dielectric Constant and Atomic Surface Tensions, *J. Phys. Chem. B*, 2009, **113**, 6378–6396.

9 (*a*) K. Fukui, The Path of Chemical Reactions - The IRC Approach, *Acc. Chem. Res.*, 1981, **14**, 363–368; (*b*) H. P. Hratchian and H. B. Schlegel, Accurate reaction paths using a Hessian based predictor-corrector integrator, *J. Chem. Phys.*, 2004, **120**, 9918–9924.

10 Y. Zhao and D. G. Truhlar, The M06 suite of density functionals for main group thermochemistry, thermochemical kinetics, noncovalent interactions, excited states, and transition elements: two new functionals and systematic testing of four M06-class functionals and 12 other functionals, *Theor. Chem. Accounts*, 2008, **120**, 215–241.

11 (*a*) NCIWEB is a web implementation of the NCIPLOT code. It provides a representation of the non-covalent interactions of a system based on the reduced density gradient of the electron density, It is available at, **https://lct-webtools.sorbonne-universite.fr/nciweb/index.php**; (*b*) J. Contreras-García, E. R. Johnson, S. Keinan, R. Chaudret, J.-P. Piquemal, D. N. Beratan and W. Yang, NCIPLOT: A Program for Plotting Noncovalent Interaction Regions, *J. Chem. Theory Comput.*, 2011, **7**, 625–632; (*c*) T. Novoa, R. Laplaza, F. Peccati, F. Fuster and J. Contreras-García, The NCIWEB Server: A Novel Implementation of the Noncovalent Interactions Index for Biomolecular Systems, *J. Chem. Inf. Model.*, 2023, **63**, 4483–4489; (*d*) For more information about NCIPLOT, see: **https://www.lct.jussieu.fr/pagesperso/contrera/nci-programs.html**.

12 Ellman reported (reference 2) that when a solution of EtMgBr in Et$_2$O was added to a solution of (*R*)-*N*-benzylidene-2-methylpropane-2-sulfinamide in CH$_2$Cl$_2$ cooled to −48 °C, the diastereomeric ratio of the addition

products $(R_S,S):(R_S,R)$ was 92:8. Please note that imine **1** in Scheme 1 has the (*S*) absolute configuration, which implies that the enantiomers of the addition products would be formed in the reaction under study in comparison with Ellman's results.

13 The images of all the molecular structures have been done with the program: R. Dennington, T. Keith and J. Millam, *GaussView 6*, Semichem Inc., Shawnee Mission, KS, 2019.

14 Throughout this manuscript, bold numbers with ' have been used to label species that have an s-*cis* conformation of the C═N and S═O bonds.

15 The conformational issues of the Et_2O molecule in the structures that contain one were studied by performing successive relaxed PES scans modifying the CH_2–O–CH_2–CH_3 dihedral angles of that molecule.

16 Magnesium atom has shown to be able to coordinate to more than four ligands. See, for instance: (*a*) E. C. Ashby and W. E. Becker, Concerning the Structure of the Grignard Reagent, *J. Am. Chem. Soc.*, 1963, **85**, 118–119; (*b*) J. Tammiku-Taul, P. Burk and A. Tuulmets, Theoretical Study of Magnesium Compounds: The Schlenk Equilibrium in the Gas Phase and in the Presence of Et_2O and THF Molecules, *J. Phys. Chem. A*, 2004, **108**, 133–139; (*c*) J.-L. Ye, P.-Q. Huang and X. Lu, Mechanism for the

17 M. Hajji, N. Abad, M. A. Habib, S. M. H. Elmgirhi and T. Guerfel, Computational chemistry methods for modelling non-covalent interactions and chemical reactivity- An overview, *J. Indian Chem. Soc.*, 2021, **98**, 100208.

18 (*a*) F. M. Bickelhaupt, Understanding reactivity with Kohn–Sham molecular orbital theory: E2–SN2 mechanistic spectrum and other concepts, *J. Comput. Chem.*, 1999, **20**, 114–128; (*b*) D. H. Ess and K. N. Houk, Distortion/Interaction Energy Control of 1,3-Dipolar Cycloaddition Reactivity, *J. Am. Chem. Soc.*, 2007, **129**, 10646–10647; (*c*) I. Fernández and F. M. Bickelhaupt, The activation strain model and molecular orbital theory: understanding and designing chemical reactions, *Chem. Soc. Rev.*, 2014, **43**, 4953–4967.

19 Cartesian coordinates of the optimized structures and energy values obtained after performing the DFT calculations at 225.15 K are included in the SI.

20 A preliminary report was deposited in the preprint repository ChemRxiv: D. Guijarro, *ChemRxiv*, 2024, preprint, DOI: **10.26434/chemrxiv-2024-rz7bc**.

Regioselective Asymmetric Addition of Grignard Reagents to Malimides: A Computational Exploration, *J. Org. Chem.*, 2007, **72**, 35–42.